Experimental and Modeling Results of Mixture Optimization of a Mixed Gas Joule-Thomson Cycle

J. Detlor, J. Pfotenhauer, and G. Nellis

University of Wisconsin-Madison, Department of Mechanical Engineering
Madison, WI 53706, USA

ABSTRACT

This paper describes the experimental investigation and development of a computational tool that is used to optimize the gas mixture composition for a Joule-Thomson (JT) cycle for specified operating parameters. A mixture optimization model was previously developed that is capable of determining optimal three-component mixtures based on the analysis of the maximum value of the minimum isothermal enthalpy change, Δh_T, that occurs over the operating temperature range coupled with an evaluation of the fraction of the heat exchanger that exists in a two-phase state within that range. This paper highlights the design and construction of a prototype mixed gas JT cryocooler built to investigate mixture selection and verify the modeling tool, particularly in the 120-150K cold-end temperature range. The prototype has operated while charged with several gas mixtures over a range of operating pressures and pressure ratios. The experimental mass flow rate, temperature at the outlet of the JT valve, and cooling load are compared to the expected values based on the mixture optimization model. The lowest cold-end temperature to date is 175K. Current efforts are directed at increasing the pressures and pressure ratios that the test facility is capable of providing. Once updated, the JT cryocooler will be able to reach the lower cold-end temperatures desired and these results will be used to further refine the model to enable mixture optimization as well as cryostat design.

INTRODUCTION

Small closed-cycle Joule-Thomson (JT) cryocoolers are used in a variety of applications ranging from cryosurgery to the cooling of sensors. They are attractive due to their small size, fast cool-down time and low vibration [1,2]. Nonetheless, the use of small closed-cycle JT cryocoolers has been limited due their relatively low thermodynamic efficiency at typical cryogenic device temperatures. For the cycle to achieve an increased efficiency that is comparable to that of Stirling-cycle coolers while continuing to use low cost compressors, it is necessary that the JT cycle provide cooling at low pressure ratios and low values of operating pressures [3]. A suitable mixture can provide an increased cooling load while enabling the operation at much lower pressures and pressure ratios than would be possible with a pure fluid [4]. However, selecting a properly suitable mixture for a mixed gas JT cycle is a challenging design problem.

A MATLAB™ program was previously developed which is capable of determining optimal three-component mixtures based on the analysis of the maximum value of the minimum isothermal

Cryocoolers 21, edited by R.G. Ross, Jr., J.R. Raab and S.D. Miller

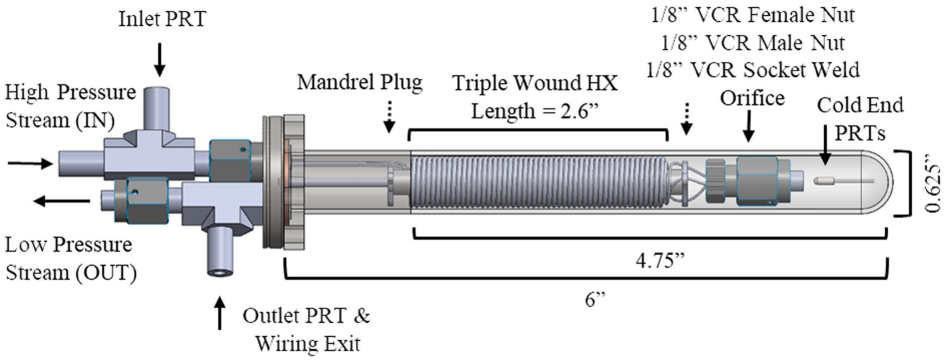

Figure 1. A SOLIDWORK CAD software rendering of the JT cryocooler prototype. Not shown for rendering simplicity is the winding technique performed to construct the heat exchanger.

enthalpy change, Δh_T, that occurs over the operating temperature range coupled with an evaluation of the percent of the heat exchanger that exists in a two-phase state within that range [5,6,7]. The program has been updated to limit the molar fraction of a component based upon the experimental charge pressure and the saturated vapor pressure of the component at room temperature to ensure that a single-phase gas is used to charge the cryocooler. The model has been exercised for flammable and non-flammable mixtures as presented in previously published work and in this paper [6,7,8]. A JT cryocooler prototype has been assembled to experimentally validate the modeling results. The cryocooler design and construction are detailed in the following.

CRYOCOOLER DESIGN AND CONSTRUCTION

A prototype JT cryocooler has been constructed to further investigate optimal mixture selection, particularly in the 120-150K cold-end temperature range. A Solidworks™ CAD software rendering of the cryocooler is shown in Fig. 1.

G10 Mandrel

The high pressure stream enters the cryocooler and splits into three finned copper tubes that are helically coiled around a hollow G10 mandrel that is filled with polystyrene foam. The G10 mandrel has an inner and outer diameter of 0.25" and 0.187", respectively, and is closed at both ends by stainless steel mandrel plugs shown in Fig. 2. The mandrel plugs provide structure for the assembly of the heat exchanger while eliminating the flow path through the G10 mandrel. The wir-

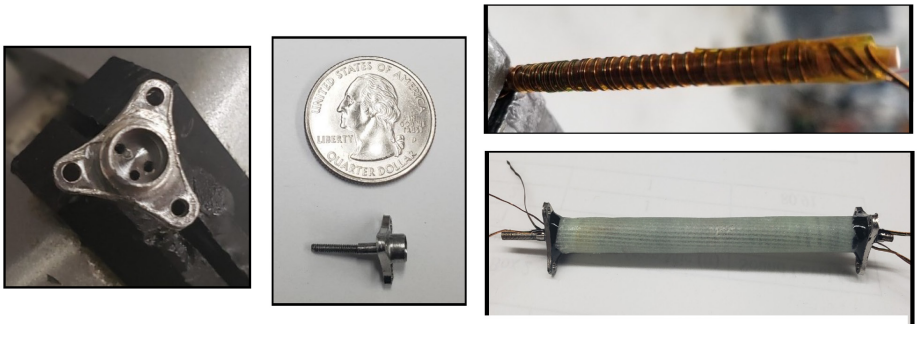

Figure 2. Mandrel plugs (left) and PRT wiring inside mandrel and assembled G10 mandrel (right).

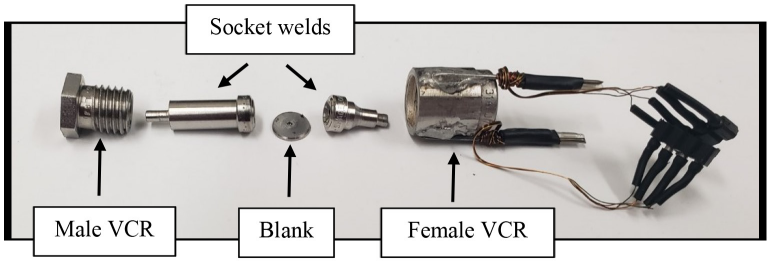

Figure 3. JT orifice assembly.

ing for the cold end platinum resistance thermometers (PRTs) run through the mandrel plugs and G10 mandrel to the outlet of the ConFlat end plate. Fig. 2 shows the PRT wiring inside the mandrel as well as the assembled G10 mandrel.

JT Orifice

The three finned heat exchanger tubes merge back into one flow path at the JT valve. The JT orifice consists of a 1/8" blank with either a small diameter hole in its center or a ruby jewel orifice epoxied into a counter bore in the blank. The orifice is held in position by 1/8" VCR female and male nuts. The JT orifice assembly is shown in Fig. 3. The low pressure stream then returns to the outlet of the ConFlat end plate by flowing over the fins on the outside of the finned tubes. The heat exchanger and JT valve are enclosed by a 5/8" Kovar-to-7052 glass domed adapter. The overall length of the heat exchanger and cryocooler are 2.6" and 6", respectively.

Heat Exchanger

The finned heat exchanger tubing has inner, outer, and finned diameters of 0.012", 0.02" and 0.04", respectively. The length of each finned heat exchanger tube is 60". The design of the three finned heat exchanger tubes wound around the G10 mandrel was given much consideration. To reduce the possibility of flow mal distribution in the high pressure stream between the three parallel tubes and avoid the resultant performance deterioration, the length of each finned heat exchanger tube should be the same. If the length of the tube is not equal then shorter tubes would offer lower resistance and carry a higher flow rate [9]. To maintain uniform flow of the low pressure stream, the radial spacing of the finned heat exchanger tubes and the separating monofilament line is as uniform as possible from the mandrel to the inner surface of the glass dome. This avoids flow non uniformity over the cross-section of the heat exchanger which would otherwise occur when the flow preferentially follows the path with the widest spacing [9].

To maintain equal tube length, wound length and radial spacing, the inner and outer layers of the finned heat exchanger tubing are swapped three times on the G10 mandrel during construction. The middle layer of tubing remains in the middle throughout. An illustration of the cross-over technique (the length of the cross-over has been greatly exaggerated for illustrative purposes) and pictures of the prototype heat exchanger winding are shown in Fig. 4. Each layer of finned heat exchanger tubing is wound in opposite directions with a layer of Teflon tape placed in between to assist with monofilament line placement on each layer. Additional Teflon tape is wrapped around the outside of the heat exchanger to create a snug fit with the glass dome. A wound length of 2.6" and inner and outer diameter of 0.22" and 0.52", respectively, were chosen for the heat exchanger based on available sizes for the glass domed adapter and simple calculations for the targeted conductance.

Temperature Sensors

The cryocooler is equipped with five PT-111 Lake Shore Cryotronics PRTs to measure the stream temperatures at the inlet and outlet of the cryocooler exit of the JT orifice, and the outside of the glass dome at the cold-end. There are two PRTs installed in-stream at the exit of the JT ori-

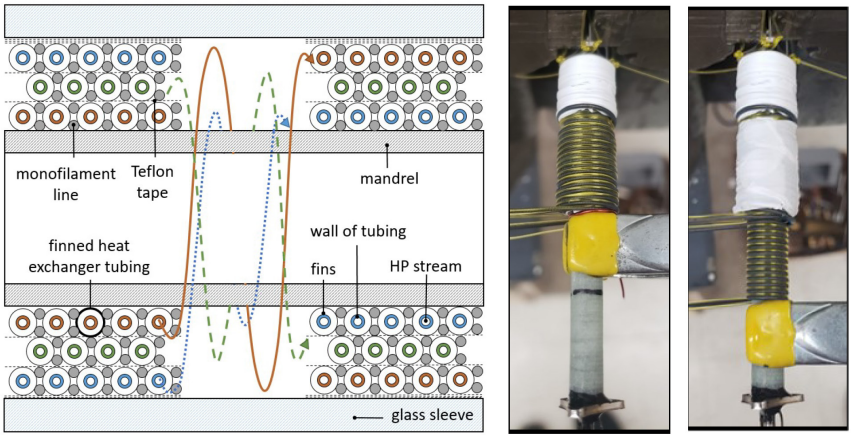

Figure 4. Visualization of the winding technique used to construct the helically coiled heat exchanger (left) and a pictures of the winding during construction (right).

fice to characterize the cold-end temperature. The PRTs are pictured in Fig. 5. The assembled JT cryocooler prototype is shown in Fig. 6.

EXPERIMENTAL RESULTS

The prototype cryocooler has been operated while charged with a selection of flammable, semi-flammable and non-flammable mixtures composed of argon, ethane, krypton methane, nitrogen, R14, R23, R32, R125 and R134a. Details regarding the test facility (e.g., compressor, charging station, gas chromatograph, etc.) can be found in the previously published work [7]. The temperatures

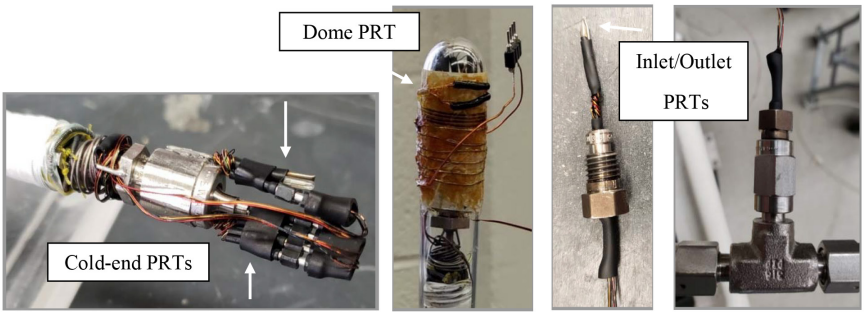

Figure 5. PRTs installed on cryocooler

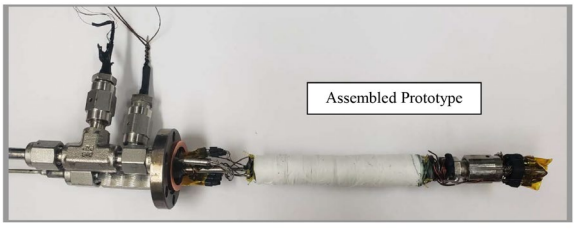

Figure 6. Assembled JT cryocooler prototype shown without glass dome adapter enclosure.

at the cold-end, on the dome and at the inlet and outlet were measured as well as the pressures at the inlet and outlet. Various sizes of the JT orifices were installed ranging from 0.0025" to 0.011" in diameter. Mass flow rates recorded ranged from 0.107 g/s to as low as 0.010 g/s. The subsequent sections will present the cold-end temperature as a function of JT orifice size for a selected mixture with operating pressures of 50-150 psia and the associated inferred parasitic loss of the cryocooler.

Variable JT Orifice

Values of the cold-end temperature were collected and compared for the mixture characterized by the Δh_T vs T plot shown in Fig. 7 while the JT orifice size was varied. The size of the JT orifice, mass flow rate and minimum cold-end temperature for each run is indicated in Fig. 7 and plotted upon the isothermal enthalpy difference for the mixture as a function of load temperature from the mixture optimization model. As the size of the JT orifice is reduced from 0.011" to 0.003", the mass flow rate decreases from 0.107 g/s to 0.014 g/s. The cold-end temperature decreases with mass flow rate until an optimal mass flow rate is achieved, after which the cold-end temperature begins to rise with ***any*** further reduction of the mass flow rate. The black dashed line located at approximately 204K on Fig. 7 is the temperature at which the value of Δh_T reaches a minimum and therefore is the temperature that limits the cooling capacity for this mixture. It is observed that as the optimal mass flow rate is approached, so too is this limiting temperature.

Cryocooler Loss

The loss for the cryocooler (which includes both parasitic heat transfer and heat exchanger loss) can be estimated as the product of the mass flow rate and the minimum value of the Δh_T over the temperature range of the experimental run. The loss is also indicated for each run in Fig. 7. If the heat exchanger was performing ideally (i.e., the heat exchanger loss was zero) then the loss would be equal to the parasitic heat load associated with conduction and radiation. This heat load increases with decreasing cold-end temperature. However, this is not the trend observed in Fig. 7 because the ineffectiveness and pressure drop loss associated with the heat exchanger both tend to decrease as the flow rate is reduced. Therefore, as the mass flow rate decreases the value of the heat exchanger loss is reduced but the value of the parasitic heat loss is increased. The values of the loss at very low temperature will tend to approach the parasitic heat loss while the values at high temperature will approach the heat exchanger loss. In this way it is possible to approximately delineate these two loss mechanisms.

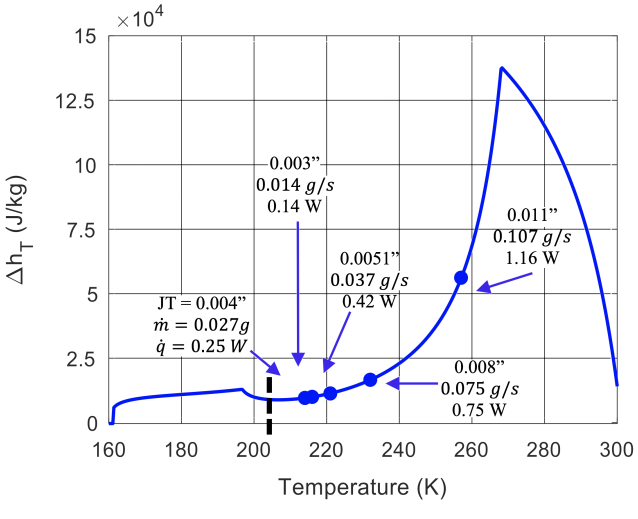

Figure 7. Visualization of experimental results and parasitic loss for 20% R14, 16% R23 and 64% R134a while varying JT orifice size

INCREASED OPERATING PARAMETERS

The cryocooler is currently operating at pressures, pressure ratios and flow rates that are targeted as the baseline achievable operating parameters for the application that motivates this research. However, the cold-end temperature is significantly warmer than the target cold-end temperature. With operating pressures of 50-150 psia and a pressure ratio of 3, the lowest cold-end temperature achieved by the cryocooler was 204K with a mixture of 20% R14, 75% R32 and 5% R125 on a molar basis. Additional gas mixtures with alternative components and compositions will continue to be tested in this range of operation. However, to reach lower cold-end temperatures and further the investigation of mixture selection, increased operating pressures and pressure ratios must be tested.

Mixture Optimization Results for Increased Operating Pressures and Pressure Ratios

Mixture optimization was performed for flammable and non-flammable mixtures for three sets of suction and discharge pressures: 50 and 150 psia, 40 and 160 psia, and 75 and 225 psia. This allows for a comparison between a set of suction and discharge pressure that have the same pressure ratio but different operating pressures and those with the same approximate operating pressure but different pressure ratios. The fluids included in the analysis for the flammable mixture optimization are argon, butane, isobutane, ethane, methane, pentane, propane, and nitrogen. The fluids included in the analysis for the non-flammable mixture optimization are argon, R14, R23, R116, R134a, R218, krypton and nitrogen. All mixtures were analyzed for load temperatures ranging from 110-180 K in increments of 10 K while the supply temperature remained constant at 300 K.

Figure 8 illustrates the refrigeration per mass flow, $\dot{Q}/\dot{m}$, as a function of load temperature for the three sets of suction and discharge pressures. Each marker represents the maximum value of the minimum $\dot{Q}/\dot{m}$ that occurs for the optimal combination of three fluids and is related to composition that is selected specifically for that load temperature (i.e. these curves should not be interpreted as load curves for a specific mixture but

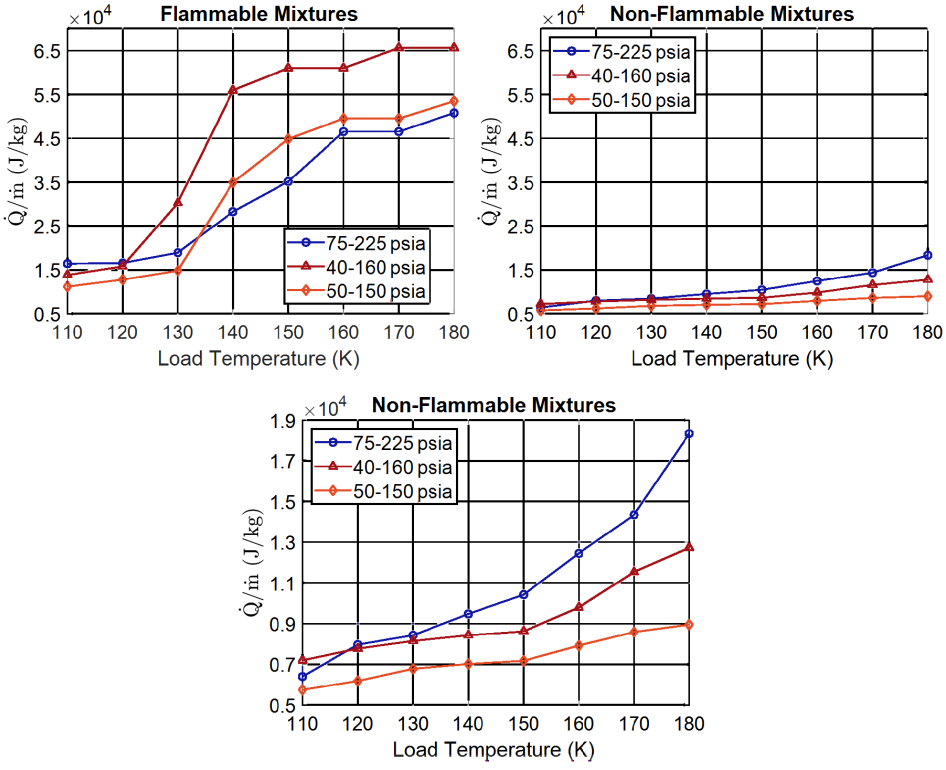

Figure 8. Refrigeration per mass flow as a function of load temperature for various pressure ratios and operating pressures.

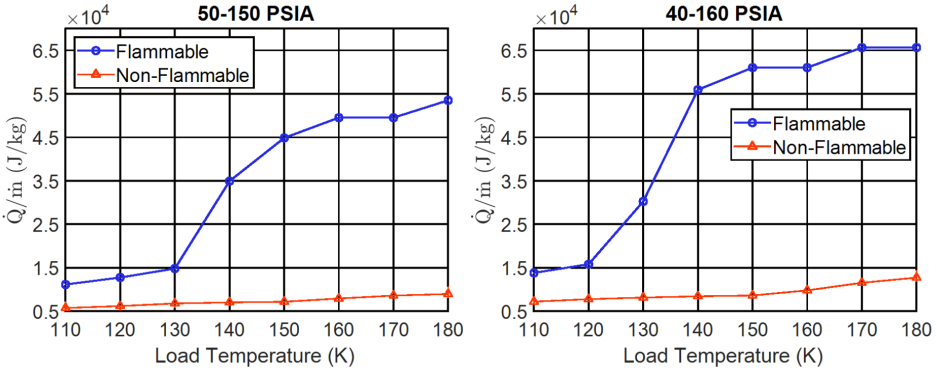

Figure 9. Refrigeration per mass flow rate as a function of load temperature for 50-150 psia and 40-160 psia.

rather as the absolute maximum potential of all combinations of three fluids considered). The refrigeration per mass flow rate for the non-flammable mixtures shown in the upper right of Fig. 8 is scaled for easy comparison with the flammable mixtures while the same plot is shown again on the bottom with an alternative scale to allow for better viewing of the trend lines.

For the non-flammable optimal mixtures, suction and discharge pressure of 75-225 psia produce the greatest values of $\dot{Q}/\dot{m}$ for load temperatures of 120 K and above while pressures of 50-150 psia produce the lowest values. Thus, within the target operating parameters, it is important to increase the operating pressures and pressure ratio in order to obtain a non-flammable mixture with the greatest value of $\dot{Q}/\dot{m}$.

This trend is not observed for the flammable mixtures. Suction and discharge pressures of 75- 225 psia produce the lowest values of $\dot{Q}/\dot{m}$ for load temperatures of 140 K and above while suction and discharge pressures of 40-160 psia produce the greatest values of $\dot{Q}/\dot{m}$ for load temperatures of 120 K and above. This is due to limitations on the mixture composition imposed by the requirement of a single-phase gas at charge pressure. Therefore, within these operating parameters, it is more beneficial to increase the pressure ratio rather than the operating pressures to obtain a flammable mixture with the greatest value of $\dot{Q}/\dot{m}$. As a result, it is expected that for optimal semi-flammable mixtures there will be a flammability limit when increasing the pressure ratio is more beneficial than increasing the operating pressures.

It is also significant to note the magnitudes of $\dot{Q}/\dot{m}$ in Fig. 8. For the flammable mixtures, the value of $\dot{Q}/\dot{m}$ is reduced by over half moving from the optimal mixture at a load temperature of 140 K to the optimal mixture at a load temperature of 120 K for suction and discharge pressures of 50-150 psia. For suction and discharge pressure of 40-160 psia, the value of $\dot{Q}/\dot{m}$ is reduced by over 70% moving from 140 K to 120 K. This illustrates the difficulty of finding a mixture that will produce cooling at load temperatures below 140 K. Furthermore, the values of $\dot{Q}/\dot{m}$ for the optimal non-flammable mixtures are significantly lower than the values for the optimal flammable mixtures. This is shown most clearly in Fig. 9. $\dot{Q}/\dot{m}$ only approaches similar values for load temperatures of 130 K and below, and even for these load temperatures the values of $\dot{Q}/\dot{m}$ for the optimal flammable mixtures are approximately double the values of $\dot{Q}/\dot{m}$ for the optimal non-flammable mixtures. A similar trend was observed for suction and discharge pressures of 75-225 psia.

Updates to the Experimental Test Facility

Experimental testing is limited by the range of operating parameters that the test facility is capable of providing. Current work is underway to extend the range of these operating parameters. Updates to the test facility include: addition of a second compressor, installation of a new aftercooler with higher maximum operating pressure, and installation of electric heaters both before the first compressor and at the inlet of the cryocooler. A schematic of the updated facility is shown in Fig. 10.

These updates will allow testing of operating pressures and pressure ratios discussed in the previous section. The operating parameters will be limited by a maximum suction pressure (and charge pressure) of 150 psia and maximum pressure ratio of 6:1. During updates, the test facility was charged with 20% R14, 75% R32 and 5% R125 on a molar basis (the same mixture that reached 204 K with suction and discharge

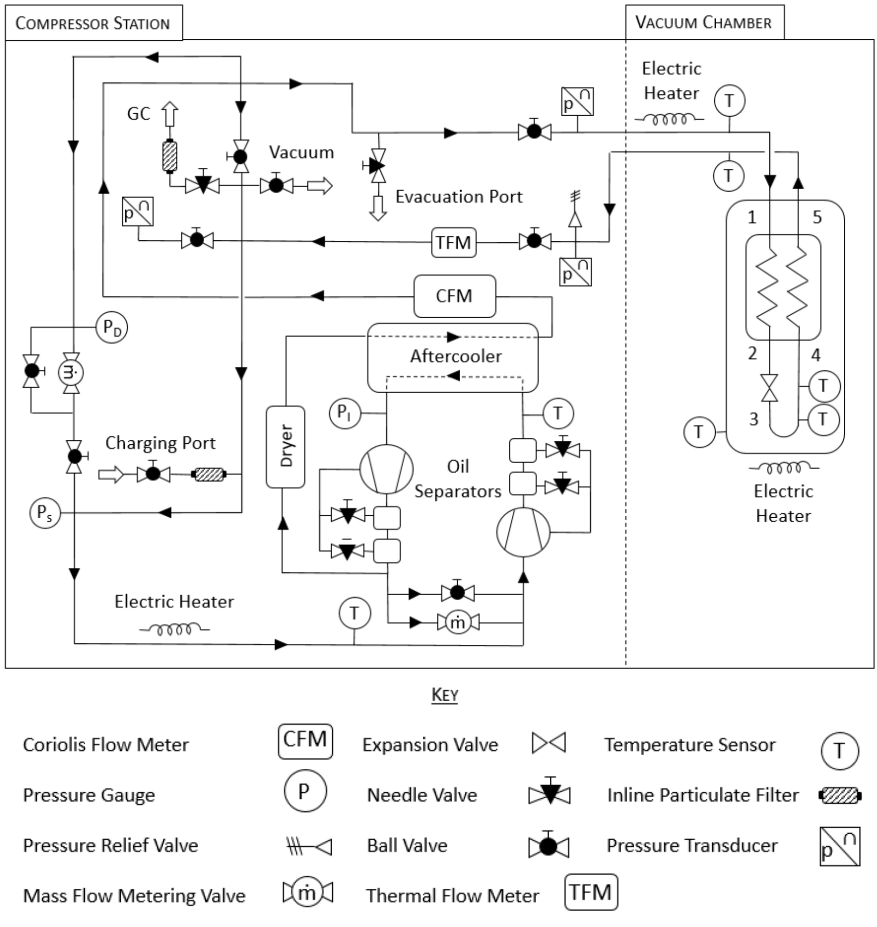

Figure 10. Schematic of experimental test facility.

pressures of 50-150 psia). With operating pressures of 75-205 psia, this mixture was able to reach a cold-end temperature of 175 K. Future operation with optimally selected mixtures for these operating parameters and temperature range will allow the cryocooler to reach lower cold-end temperatures.

CONCLUSION

The primary objective of this research is to develop and experimentally validate a computational tool that can optimize the gas mixture composition for a JT cycle that spans a specified temperature range for given values of operating pressures, pressure ratios, and flow rates. A mixture optimization model was previously developed and is currently being refined through experimental testing of a JT cryocooler prototype. While the cryocooler is currently operating at pressures, pressure ratios, and flow rates that are consistent with the operating parameters associated with the application that motivated this research, the cold-end temperature is significantly warmer than the target cold-end temperature. The test facility is therefore currently being updated to provide higher operating pressures and pressure ratios in order to allow the cryocooler to reach lower cold-end temperatures.

Future plans include updates to the mixture optimization model, development of a more detailed heat exchanger model and further experimental testing. The heat exchanger model will consider the effect of operating parameters, geometry, mixture composition, and quality on the conductance and pressure loss. This will make it possible to provide more accurate predictions of mixture performance and thus aid in the selection of mixtures with better real world performance.

REFERENCES

1. Little, W. A., "Microminiature refrigeration," *Review of Scientific Instruments*, vol. 55, no. 5 (1984), pp. 661-680.
2. Maytal, B.-Z., and Pfotenhauer, J. M., *Miniature Joule-Thomson Cryocooling: Principles and Practice*, Springer, New York (2013).
3. Olson, J. R., Roth, E., Guzinski, M., Ruiz, A., Mangun, C. L., King, D., Hejmanowski, N., and Carroll, D. L., "Joule-Thomson microcryocooler test results," *Cryocoolers 20*, ICC Press, Boulder, Colorado (2018) pp. 287-294.
4. Hinze, J., "Thermodynamic optimization of mixed refrigerant Joule-Thomson cycle with heat transfer considerations," (Madison: Univ. of Wisc. Madison) MS [thesis] Available from: UW Madison Library System.
5. *MATLAB release R2019b*, The MathWorks, Inc., Natick, Massachusetts, United States.
6. Detlor, J., Pfotenhauer, J., and Nellis, G., "Mixture optimization for mixed gas Joule-Thomson cycle," *IOP Conf. Ser: Mater. Sci. Eng, Vol. 278* (2017) 012045.
7. Detlor, J., Pfotenhauer, J., and Nellis, G., "Experimental investigation of mixture optimization for mixed Joule-Thomson cycle," *Cryocoolers 20*, ICC Press, Boulder, Colorado (2018), pp. 305-316.
8. Detlor, J., Gruenstern, R., Pfotenhauer, J., and Nellis, G., "Experimental validation and refinement of mixture optimization for a mixed gas Joule-Thomson cycle," *IOP Conf. Ser: Mater. Sci. Eng, Vol.* 755 (2020) 012019.
9. Barron, R. F., and Nellis, G., *Cryogenic Heat Transfer*, CRC Press (2017).